



**Potential sources and processes affecting speciated atmospheric mercury at  
Kejimikujik National Park, Canada**

Xiaohong Xu<sup>1\*</sup>, Yanying Liao<sup>1</sup>, Irene Cheng<sup>2</sup>, Leiming Zhang<sup>2\*</sup>

<sup>1</sup> Department of Civil and Environmental Engineering, University of Windsor, 401 Sunset  
Avenue, Windsor, Ontario, N9B 3P4, Canada

<sup>2</sup> Air Quality Research Division, Science and Technology Branch, Environment and Climate  
Change Canada, 4905 Dufferin Street, Toronto, Ontario, M3H 5T4, Canada

Corresponds to Xiaohong Xu ([xxu@uwindsor.ca](mailto:xxu@uwindsor.ca)) or Leiming Zhang ([leiming.zhang@canada.ca](mailto:leiming.zhang@canada.ca))



1 **Abstract:** Source apportionment analysis was conducted with Positive Matrix  
2 Factorization (PMF) and Principal Component Analysis (PCA) methods using  
3 concentrations of speciated mercury (Hg), i.e., gaseous elemental mercury (GEM),  
4 gaseous oxidized mercury (GOM), and particulate-bound mercury (PBM), and other  
5 air pollutants collected at Kejimikujik National Park, Nova Scotia, Canada in 2009 and  
6 2010. The results were largely consistent between the two years for both methods. The  
7 same four source factors were identified in each year using PMF method. In both  
8 years, factor Photochemistry and Re-emission had the largest contributions to  
9 atmospheric Hg, while the contributions of Combustion Emission and Industrial  
10 Sulfur varied slightly between the two years. Four components were extracted with air  
11 pollutants only in each year using PCA method. Consistency between the results of  
12 PMF and PCA include, 1) most or all PMF factors overlapped with PCA components,  
13 2) both methods suggest strong impact of photochemistry, but little association  
14 between ambient Hg and sea salt, 3) shifting of PMF source profiles and source  
15 contributions from one year to another was echoed in PCA. Inclusion of  
16 meteorological parameters led to identification of an additional component - Hg Wet  
17 Deposition in PCA, while it did not affect the identification of other components.

18 The PMF model performance was comparable in 2009 and 2010. Among the  
19 three Hg forms, the agreement between predicted and observed annual mean  
20 concentrations were excellent for GEM, very good for PBM and acceptable for GOM.  
21 However, on daily basis, the agreement was very good for GEM, but poor for GOM  
22 and PBM. Sensitivity tests suggest that increasing sample size by imputation is not  
23 effective in improving model performance, while reducing the fraction of  
24 concentrations below method detection limit, by either scaling GOM and PBM to  
25 higher concentrations or combining them to reactive mercury, is effective. Most of the  
26 data treatment options considered had little impact on the source  
27 identification/contribution.

## 28 1. Introduction

29 Atmospheric mercury (Hg) exists in the form of gaseous elemental Hg (GEM) and  
30 oxidized Hg, the latter can be in gaseous phase (gaseous oxidized Hg - GOM) or  
31 associated with particulate matter (particulate - bound Hg - PBM). Identification of  
32 major sources and processes affecting ambient levels of different Hg forms will help



33 mitigate the risks of Hg pollution. Atmospheric Hg can be produced from  
34 anthropogenic activities, natural events and re-emission of previously deposited Hg,  
35 the latter two are sometimes grouped together as natural emission sources (Gustin et  
36 al., 2008; Pirrone et al., 2010; UNEP, 2013; Gaffney and Marley, 2014; Zhang et al.,  
37 2016). Natural events consist of volatilization from the ocean, volcanic eruption,  
38 geothermal activities, and weathering of Hg-containing minerals (Pirrone et al., 2010;  
39 Gaffney and Marley, 2014). Small scale or artisanal gold mining, mining and smelting,  
40 and coal combustion are the three major anthropogenic sources (UNEP, 2013; Zhang  
41 et al., 2016). Some of the dry and wet deposited PBM and GOM will be reduced to  
42 GEM in soil, water, and vegetation surfaces where Hg will be re-emitted in the form  
43 of GEM to the atmosphere (Gaffney and Marley, 2014). However, the contributions of  
44 each source and process to a given receptor site are affected by many factors including  
45 proximity to sources and weather conditions.

46 Various receptor-based models have been used to identify the sources and  
47 processes affecting ambient Hg levels (Cheng et al., 2015). Among these, Positive  
48 Matrix Factorization (PMF) and Principal Component Analysis (PCA) are two  
49 commonly used methods. PMF method provides quantitative source profiles and  
50 source contributions. The resultant source profiles could aid future studies in factor  
51 interpretation. Another strength of PMF is input variable screening and provision of  
52 model performance measures. The users could specify uncertainty values for each  
53 variable in each sample to reduce the impact of measurements with high uncertainties  
54 on the final results (US EPA, 2014a; Hopke, 2016). However, in order to derive  
55 profiles, PMF requires a large number of air pollutants which are often unavailable. In  
56 contrast, PCA can only provide qualitative assessment of sources/processes. One  
57 advantage of PCA over PMF is its capability of allowing inclusion of meteorological  
58 parameters as input, enabling the assessment of the effects of weather conditions on  
59 ambient Hg concentrations (Cheng et al., 2015). Therefore, it is beneficial to conduct  
60 source apportionment of atmospheric Hg using both PMF and PCA. To date, only one  
61 study used this combined approach (Cheng et al., 2009), yet it lacked a thorough  
62 comparison of the results. Furthermore, the ability of receptor models to reproduce the  
63 observed concentrations should be assessed in order to gauge the model performance  
64 (Henry, 1991; Viana et al., 2008), which has been rarely reported in the literature.



65 The overall objective of this study is to identify the factors affecting ambient Hg  
66 concentrations at a receptor site using PMF and PCA approaches. The specific  
67 objectives are to, (1) identify the factors affecting ambient Hg concentrations using  
68 PCA and PMF model; (2) summarize the similarity and differences in PMF factors  
69 and PCA components; (3) evaluate the PMF model performances by Hg forms; (4)  
70 investigate the impact of including meteorological parameters on PCA results, and (5)  
71 assess the sensitivity of PMF results and performance to different treatment of  
72 missing data and low concentration values of speciated Hg.

73

## 74 2. Method

### 75 2.1 Study site

76 The study site is located in Kejimikujik (KEJ) National Park (44.32°N; 65.2°W;  
77 elevation: 170 m), Nova Scotia, Canada. The KEJ site is one of the first speciated Hg  
78 sites operated by Environment Canada outside the Arctic. This site was selected  
79 primarily because of the bioaccumulation issues at this area. Studies have found that  
80 common loons in Kejimikujik National Park had the highest mean blood Hg  
81 concentrations in northeastern United States and Southeastern Canada (Evers et al.,  
82 2007). Similarly, a 1996/97 survey found that yellow perch and common loons from  
83 Kejimikujik National Park and National Historic Site (Nova Scotia) had the highest  
84 blood Hg concentrations across North America. A 2006/07 follow up study on yellow  
85 perch observed on average a 29% increase in 10 out of 16 lakes, although  
86 anthropogenic emission from North America decreased between the mid-90s to the  
87 mid-2000s (Wyn, 2010).

88 The sampling site was surrounded by forests on a flat terrain. It was  
89 approximately 50 km away from the nearest coast, 120 km southwest of Halifax, and  
90 relatively remote from anthropogenic air emissions. A search of the National Pollutant  
91 Release Inventory (NPRI, Environment Canada, 2016) yielded seven Nova Scotia  
92 facilities reporting Hg air releases in both 2009 and 2010. Four of them were electric  
93 power generation stations, the other three were a refinery, a cement plant, and a  
94 university. The provincial annual air emission of Hg were 147.5 kg and 90.3 kg in  
95 2009 and 2010, respectively (Table S1). The two largest Hg emitters were Lingan  
96 Power Generating Station (2009-2010 average: 71 kg/yr) and Trenton Power



97 Generating Station (26 kg/yr), located 450 km and 250 km from the sampling site,  
98 respectively. The nearest anthropogenic Hg sources (Dalhousie University, Halifax:  
99 0.17 kg/yr, Imperial oil, Dartmouth Refinery: 2.8 kg/yr) were 140 km northeast of the  
100 sampling site. In addition to Hg sources, the nearby NPRI (Environment Canada,  
101 2016) combustion/industrial sources were a biomass-fueled power station and tire  
102 production factory located approximately 50 km east/southeast of the KEJ site (Table  
103 S1).

104

## 105 2.2 Data collection

106 GEM, GOM and PBM concentrations were collected from 2009 to 2010 using  
107 Tekran<sup>®</sup> instruments (Models 1130/1135/2537) at 3-hour intervals. Hourly  
108 concentrations of ground level ozone (O<sub>3</sub>) and meteorological parameters  
109 (temperature, relative humidity, wind speed, and precipitation amount), as well as  
110 daily concentrations of SO<sub>2</sub> and HNO<sub>3</sub>, PM<sub>2.5</sub> (2009 only), and particulate SO<sub>4</sub><sup>2-</sup>, NO<sub>3</sub><sup>-</sup>,  
111 Mg<sup>2+</sup>, Cl<sup>-</sup>, K<sup>+</sup>, Ca<sup>2+</sup>, NH<sub>4</sub><sup>+</sup>, and Na<sup>+</sup> were also collected at KEJ site. Detailed  
112 information of data collection can be found in Cheng et al. (2013).

113 Hourly or 3-hr concentrations of GEM, GOM, PBM, O<sub>3</sub> and meteorological data  
114 were averaged into daily values because PMF and PCA require the same interval for  
115 all input variables. All daily values were the same as those used in a PCA study by  
116 Cheng et al. (2013). The general statistics of the daily concentrations are listed in  
117 Table 1 and Table 2 for year 2009 and year 2010, respectively. The number of missing  
118 daily concentrations ranged from 0% (ozone, 2010) to 41% (PBM, 2009), which are  
119 excluded from PMF or PCA. Among the three Hg forms, GEM had the fewest values  
120 below the Method Detection Limit (MDL), while GOM had the largest percentages of  
121 concentrations below MDL, followed by PBM, in both years. The variability, as  
122 indicated by coefficient of variability, was low for GEM but much higher for GOM  
123 and PBM.

124

## 125 2.3 Model setup and case design



126 Detailed description of the theory of PMF and PCA methods can be found in  
127 Cheng et al. (2015). Model set up and case design are described below.

128 **PMF**

129 EPA PMF5.0 (US EPA, 2014b) was used in this study. The 12 cases investigated  
130 are listed in Table 3. Two approaches were employed in PMF modeling to handle  
131 missing values. The first approach is listwise deletion. Listwise deletion excludes all  
132 the records having one or more missing values, resulting in a complete data matrix as  
133 required in PMF. However, it may cause a large reduction of the dataset when one of  
134 the pollutants has many missing values or several pollutants have missing values at  
135 different time periods. In environmental studies, this approach may lead to biased  
136 results because listwise deletion benefits the records with high concentrations when  
137 below MDL values are flagged as missing (Huang et al., 1999). The second method is  
138 imputation, which increases the sample size in PMF. Hedberg et al. (2005) found that  
139 the relative error of factor profiles decreased as the sample size increased. In this study,  
140 geometric mean and median imputation were used to minimize the undue influence of  
141 extreme values as in Pekey et al. (2004). The effects of imputation was investigated in  
142 Cases 09+Mean, 10+Mean, 09+Median, and 10+Median.

143 Cases 09+RM, 10+RM, 09-RM, and 10-RM were devised to investigate the  
144 effects of excluding or combining GOM and PBM into reactive mercury (RM) on the  
145 resultant PMF results compared with the full dataset. Uncertainties of GOM and PBM  
146 measurements are considered high (Gustin et al., 2015). It has been reported that  
147 GOM may be collected on the PBM filter thus GOM concentrations could be biased  
148 low (Lynam and Keeler, 2005). Therefore, combining GOM and PBM to RM may  
149 reduce the uncertainties (Cheng et al., 2016). RM was calculated by summing GOM  
150 and PBM when both forms of Hg are detected.

151 In Case 09ScaleRM and Case 10ScaleRM, a variable scaling factor was used to  
152 increase the GOM and PBM concentrations:

153 
$$\text{scaling factor} = \sqrt{\frac{\max(x)}{x_i}} \quad (1)$$

154

155 where  $x_i$  is the concentration of GOM or PBM in the  $i^{\text{th}}$  sample. The scaling factor is  
156 large when the concentration is low, and vice versa, but the maximum concentration is



157 unchanged.

158 Equation-based uncertainties (US EPA, 2014a) were used in this study, expressed  
159 as:

$$\begin{aligned} 161 \quad \text{Uncertainty} &= \frac{5}{6} \times MDL, \text{ when concentration} \leq MDL \\ 162 \quad \text{Uncertainty} &= \sqrt{(\text{Error Fraction} \times \text{concentration})^2 + (0.5 \times MDL)^2}, \\ 163 \quad &\text{when concentration} > MDL \end{aligned} \quad (2)$$

164

165 The MDLs used in this study are 0.1 ng/m<sup>3</sup>, 2 pg/m<sup>3</sup>, and 2 pg/m<sup>3</sup> for GEM, GOM  
166 and PBM, respectively (Tekran Inc., 2010). For RM, the MDL was assumed to be 4  
167 pg/m<sup>3</sup>. The error fractions were assumed to be 15% of concentrations for Hg forms  
168 and 10% of concentrations for other compounds. This is because most of the  
169 measured GOM and PBM concentrations have low concentrations near or below  
170 MDL as seen in Tables 1-2; thus have large uncertainties as pointed out by Croghan  
171 and Egeghy (2003). Following Polissar et al. (1998), constant uncertainties (100%,  
172 200% and 1000% of the mean/median for GEM, PBM and GOM, respectively) were  
173 used for imputed Hg concentrations, based on the uncertainty distributions of the  
174 below MDL values in the two base cases. This is to down weight the imputed values.

175 No variables or samples were excluded after input data screening to reflect all  
176 observations. No variables were down-weighted, with the exception of imputed values,  
177 because runs with and without GOM and PBM categorized as “weak” led to similar  
178 results. Other PMF input parameters include: the number of runs was set to 20 to  
179 enable stability evaluation, and the best run was used; the number of the starting seed  
180 was set to 25.

181 PMF outputs used in this study include source profiles, model performances and  
182 factor contributions. Four factors were retained in each case. The factors were  
183 interpreted based on the comparison of the major variables (>=25%) in each of the  
184 four factors to markers and source profiles in the literature, taking into consideration  
185 NPRI emission sources. Stability indexes of model runs, scaled residual plot,  
186 Obs/Pred scatter plot and Obs/Pred time series were used to evaluate the model  
187 performances for speciated Hg. The impact of each data treatment method on PMF  
188 results was assessed, taking into consideration interpretability of the factors and



189 model performance of the three Hg forms.

190

### 191 *PCA*

192 The PCA source apportionment analysis using speciated Hg in 2009 and 2010  
193 was already conducted in another study (Cheng et al., 2013). In this study, different  
194 cases were investigated, as listed in Table 4. Briefly, all compounds were included to  
195 enable comparison with PMF results (Case 2009 and Case 2010), instead of removing  
196 some air pollutants as in Cheng et al. (2013) due to a lack of correlation between those  
197 air pollutants and atmospheric Hg. Pairwise deletion of missing values in Cheng et al.  
198 (2013) was replaced with listwise deletion to be consistent with the PMF model input  
199 which must be a complete data matrix. The PCA runs were conducted using SPSS  
200 22.0 (IBM Corp., USA). Cases 09-C&M and Case 10-C&M were included to evaluate  
201 the effects of weather conditions on factor identification. The components with  
202 eigenvalues greater than 1 were retained for further analysis, following the Kaiser  
203 Criterion (Kaiser, 1960). Principal components after Varimax rotation were interpreted  
204 by comparing the major variables (loadings > 0.25) of the component with the  
205 outcomes of other studies, and by checking NPRI sources in the region (Table S1).

206

## 207 **3. Results and discussion**

### 208 **3.1 PMF - base cases**

209 In this section, only the two base cases, Case 2009 and Case 2010 are considered.

#### 210 *PMF sources*

211 Table 5 and Figures 1-2 present percent concentration of each pollutant  
212 apportioned to each of the four factors. Factor 1 was named Combustion Emission  
213 due to large contributions of  $\text{SO}_4^{2-}$  (64%) and  $\text{HNO}_3$  (54%) and a moderate  
214 contribution of GOM (31%).  $\text{SO}_2$  and  $\text{NO}_x$  are precursors of  $\text{SO}_4^{2-}$  and  $\text{HNO}_3$ ,  
215 respectively. These precursors are from combustion sources and probably oxidized  
216 during the transport from sources to receptor sites (Liu et al., 2007). The presence of  
217 GOM is consistent with the combustion emission which is one of the GOM sources  
218 (Carpi, 1997). There was little  $\text{NH}_3$  emissions from point sources near the study site  
219 (Table S1). Thus, the presence of  $\text{NH}_4^+$  (71%) should be related to the transport and  
220 transformation of  $\text{NH}_3$  from agriculture emissions as well as other physical and





221 chemical processes (e.g., aqueous phase chemistry, condensational growth, droplet  
222 evaporation) producing  $\text{NH}_4^+$  (Zhang et al, 2008; Pitchford et al., 2009). In this  
223 factor, the molar ratio of  $\text{NH}_4^+$  to  $\text{SO}_4^{2-}$  is 1.7, although some observed profiles having  
224 ratios greater than 2 (Lee et al, 1999). Ratios less than 2 suggest insufficient amount  
225 of  $\text{NH}_3$  to neutralize  $\text{H}_2\text{SO}_4$  thus  $\text{H}_2\text{SO}_4$  will react with other compounds to form  
226 sulfate (Pavlovic et al., 2006; Zhang et al., 2008). The moderate contribution of PM  
227 (42%) is consistent with the presence of particulate  $\text{SO}_4^{2-}$  and  $\text{NH}_4^+$ . Also,  $\text{SO}_4^{2-}$   
228 accounted for over 50% of PM mass (Table 1). In addition to a lack of major  
229 combustion facilities nearby (Table S1), a strong correlation between  $\text{SO}_4^{2-}$  and  $\text{NH}_4^+$   
230 (Tables S2-S3) also suggest formation of secondary aerosols. Therefore, this factor  
231 suggests transported plumes instead of fresh emissions.

232 Factor 2 was assigned to Industrial Sulfur. The major variables PBM and  $\text{SO}_2$  are  
233 indicators of coal combustion (Huang et al., 2010). The minor contributions of  $\text{HNO}_3$   
234 and  $\text{NO}_3^-$  also suggest combustion sources because their precursor,  $\text{NO}_x$ , is mainly  
235 released by combustion sources (Liu et al., 2007). However, there were no  
236 combustion sources emitting Hg compounds near the KEJ site in 2009 (Table S1).  
237 Therefore, this factor is more likely related to industrial sources in the region.

238 Factor 3 was named Photochemical Process and Re-emission of Hg due to the  
239 high contributions of ozone (72%), GEM (76%), GOM (69%), PBM (63%), and  
240 moderate contributions of  $\text{Ca}^{2+}$  (45%) and  $\text{K}^+$  (37%). The high contribution of ozone  
241 indicates an ozone rich environment, resulting in oxidation of GEM to GOM and the  
242 sequential formation of PBM (Pal and Ariva, 2004; Liu et al., 2007). Although results  
243 of recent studies show that the reaction rate of Hg and ozone has large uncertainties,  
244 the oxidation of Hg by bromine is very fast (Goodsite et al., 2004). The KEJ site is  
245 near the Atlantic, making the oxidation of Hg by bromine applicable. The presence of  
246  $\text{K}^+$  is related to soil emission or biomass burning (Andersen et al., 2007), while  $\text{Ca}^{2+}$   
247 is related to soil/crustal. The site is located in Kejimikujik National Park. Therefore, it  
248 is under the impact of soil emission, emission from the nearby biomass-fired power  
249 station (Table S1), and transported biomass combustion. It was estimated that  
250 re-emission of Hg from biomass burning and land surfaces contributed 13% and 34%  
251 of the global re-emission budget, respectively (Pirrone et al., 2010). Thus, the high  
252 contribution of GEM may be attributable to the re-emission of GEM. The emission



253 from soil and biomass combustion was also identified in the PCA study at this site  
254 (Cheng et al., 2013).

255 Factor 4 has high contributions of  $\text{Cl}^-$  (100%),  $\text{Mg}^{2+}$  (82%) and  $\text{Na}^+$  (86%) and  
256 moderate contributions of  $\text{Ca}^{2+}$  (31%),  $\text{K}^+$  (39%) and  $\text{NO}_3^-$  (40%). The presence of  
257  $\text{Na}^+$ ,  $\text{Mg}^{2+}$ , and  $\text{Cl}^-$  indicates marine aerosols because these elements are rich in sea  
258 water (Huang et al., 1999). The strong correlations among these three compounds  
259 ( $\geq 0.89$ , Tables S2-S3) also suggest a common source. As the sampling site is located  
260 near the Atlantic, the presence of marine aerosols is reasonable. Major production  
261 pathways of  $\text{NO}_3^-$  include reaction of  $\text{HNO}_3$  with  $\text{NH}_3$ , sea salt and soil dust  
262 (Pakkanen, 1996). In this factor, the  $\text{NO}_3^-$  is probably related to the reaction of  $\text{HNO}_3$   
263 and sea salt. Thus, this factor was named Sea Salt.

264 As seen in Table 5 and Figures 1-2, the same four factors were identified in year  
265 2009 and 2010. The profiles of each factor were also largely consistent between the  
266 two years. Factor 1 in 2010 is similar to the factor named Combustion Emission in  
267 Case 2009. However, this factor lacks PM (not available in 2010) and has a higher  
268 contribution from  $\text{K}^+$ , which may relate to biomass burning. This factor is assigned to  
269 the same name as in 2009 because the presence of  $\text{SO}_4^{2-}$  and  $\text{HNO}_3$  is enough to  
270 identify combustion process (Liu et al., 2007). It should be noted that this factor has a  
271 much smaller constitution of GOM than in 2009. This may be due to a large reduction  
272 in  $\text{SO}_2$  emissions (2.42 million tons or 32% reduction) from coal-fired power plants  
273 across the United States between 2008 and 2010 (US EPA, 2011). Large reductions in  
274 Hg (-39%) and  $\text{SO}_2$  (-35%) emissions also occurred in Nova Scotia between 2009 and  
275 2010, as seen in Table S1. However, reduction in Hg emissions is only reflected on  
276 GOM (-75%), while GEM decreased a little and PBM increased slightly.

277 The major variables of factor 2 are also similar to those of the factor Industrial  
278 Sulfur in Case 2009. However, this factor has a moderate contribution of GOM  
279 instead of PBM in 2009. Factor 3 has similar major variables as the factor named  
280 Photochemistry and Re-emission in Case 2009. Factor 4 is dominated by  $\text{Cl}^-$  (100%),  
281  $\text{Na}^+$  (83%) and  $\text{Mg}^{2+}$  (75%). This factor was named Sea Salt as in Case 2009.

#### 282 *PMF source contributions*

283 The PMF factor contributions of the two base cases are presented in Table S4  
284 (Case 2009) and Table S5 (Case 2010). In both years, factor Photochemistry and



285 Re-emission had the largest contributions to GEM (averaging 77% and 79% in 2009  
286 and 2010, respectively), GOM (70% and 67%), and PBM (69% and 80%) among all  
287 four factors. In other words, ambient Hg concentrations at the KEJ site were  
288 dominated by photochemistry and re-emission of Hg. Industrial Sulfur had moderate  
289 contributions to GOM (average, 29%) in 2010 instead of PBM in 2009 (21%).  
290 Combustion Emission contributed 25% of GOM in 2009 but 11% each of GEM and  
291 PBM in 2010. The factor Sea Salt only had minor contribution to GEM (14% in 2009  
292 and 9% in 2010) and PBM (<10% in both years). This is not unexpected because  
293 GEM is likely to be oxidized to GOM by the *in situ* photochemical process under the  
294 bromine-rich environment (Obrist et al., 2011). However, this factor has no  
295 contribution to GOM because it was estimated that >80% of GOM in the marine  
296 boundary layer is absorbed by sea salt aerosols and it is sequentially deposited onto  
297 the earth's surface where evasion occurs (Holmes et al., 2009).

#### 298 ***PMF model performance***

299 Among the three Hg forms, GEM had the best performances in terms of scaled  
300 (i.e. standardized) residual because it had normal distribution and fewer absolute  
301 values of scaled residual greater than 3 in both years (Case 2009 and Case 2010, Table  
302 6). Table 6 also lists the coefficient of determination ( $R^2$ ) and the slope of the  
303 regression line for speciated Hg in Obs/Pred scatter plot (Figures S1-S2), to evaluate  
304 the overall model-measurement agreement. Between the two years, the agreement was  
305 better with GEM in 2010 and PBM in 2009 because of higher  $R^2$  values and slope  
306 closer to 1. The low values of  $R^2$  and slope in both years indicate the agreement was  
307 poor for GOM.

308 The Obs/Pred time series of the three Hg forms reveal the model's ability to  
309 reproduce the observational concentrations on a day-to-day basis. In Case 2009, the  
310 Obs/Pred time series (Figure S3) were split into three time periods by the data gaps,  
311 January to February (period 1), March to July (period 2), and October to December  
312 (period 3). GEM had better performances than the other two forms because the peak  
313 values were reproduced by the model in all three periods. However, the modeled  
314 values in period 3 are too low compared to observed concentrations, leading to a  
315 lower  $R^2$  (Table 6). The performance for PBM is better than GOM because the  
316 predicted concentrations tracked the observed concentrations well in period 2.



317 However, PBM concentrations were underestimated and overestimated by the model  
318 in period 1 and period 3, respectively. The GOM concentrations were not reproduced  
319 well with unmatched peak values in period 2, and there was a clear separation of  
320 observed and predicted trend lines in periods 1 and 3, leading to over prediction.

321 In Case 2010, the time series (Figure S4) were split into two periods,  
322 January-June (period 1) and July-December (period 2), based on a clearly visible  
323 overestimation of GOM concentrations in the second period. The predicted GEM  
324 concentrations tracked the trend of observations well in both periods but with more  
325 fluctuations. The model was unable to reproduce high GOM concentrations in period  
326 1. For PBM, the predicted concentration was rather flat, missing completely the high  
327 concentration episode in spring 2010.

328 The model-measurement agreement was further quantified with the ratios of  
329 predicted to observed concentrations (Pred/Obs ratio, Figure 3). In both years, the  
330 predicted GEM agreed well with the observed concentrations as supported by the  
331 small range of Pred/Obs ratios (0.56-1.32 in 2009, 0.42-1.43 in 2010) and mean ratios  
332 approaching 1 (0.97 and 0.98). On an annual basis, the observed GEM concentrations  
333 were also well reproduced because the ratios of predicted to observed annual means  
334 (annual Predmean/Obsmean) were almost 1 (0.97 and 0.98) (Tables S4-S5).  
335 Compared with GOM, PBM had better agreement between the predicted and observed  
336 concentrations with a smaller range of Pred/Obs ratios (0.40-13.4 and 0.14-18.3 vs.  
337 0.13-53 and 0-193) and mean ratios closer to 1 (2.09 and 1.98 vs. 5.89 and 4.44). In  
338 spite of large sample to sample variability in the Pred/Obs ratios, the model  
339 performance was very good for PBM (annual Predmean/Obsmean ratio of 1.03 and 1)  
340 and reasonable for GOM (0.86 and 1.34) in reproducing annual means.

#### 341 ***Comparison between PMF in year 2009 and 2010***

342 Overall, the interpretability of the factors was similar in the two years. The same  
343 factors were observed in 2009 and 2010, and most factor contributions were highly  
344 consistent between the two years. Among the three Hg forms, PMF reproduced GEM  
345 concentrations well in both years. Possible reasons of poor performance on PBM and  
346 GOM include lower concentration levels and much higher percentages of readings  
347 below MDL (Tables 1-2) leading to large uncertainties. However, the differences in



348 sample size (161 in 2009 vs. 290 in 2010) and fractions of below MDL values (Tables  
349 1-2) alone could not explain the mixed results of poor performance on GOM in 2009  
350 and PBM in 2010. Further examination of time series (Figures S3 and S4) suggests  
351 that the reduced performance could also be attributable to high concentration episodes  
352 in GOM in 2009 and PBM in 2010. The impact of Hg data treatment on PMF results  
353 was investigated and the results are presented in section 3.4.

354

### 355 **3.2 PCA components**

#### 356 *Case 09-C*

357 The component loadings of Case 09-C are presented in Table 7. PC1 was named  
358 Combustion/industrial Emission due to positive loadings of PBM, PM, O<sub>3</sub>, SO<sub>2</sub>,  
359 HNO<sub>3</sub>, Ca<sup>2+</sup>, K<sup>+</sup>, NO<sub>3</sub><sup>-</sup>, NH<sub>4</sub><sup>+</sup>, and SO<sub>4</sub><sup>2-</sup>. Most major compounds except O<sub>3</sub> were also  
360 found in a component named “transport of combustion and industrial emissions” in  
361 another PCA study using the same dataset (Cheng et al., 2013). The high loadings of  
362 secondary pollutants HNO<sub>3</sub>, NO<sub>3</sub><sup>-</sup>, and SO<sub>4</sub><sup>2-</sup> indicate the factor represents transport of  
363 combustion/industrial emission because their precursors (NO<sub>x</sub> and SO<sub>2</sub>) are mainly  
364 emitted by combustion/industrial sources (Liu et al., 2007). The precursors may be  
365 oxidized during the transport process. The moderate loading of O<sub>3</sub> is also related to  
366 the transport of combustion emission because the precursors of O<sub>3</sub> (NO<sub>x</sub> and VOC)  
367 are emitted from mobile and stationary combustion sources. Ammonia is likely related  
368 to the transport of agriculture emissions and reaction of NH<sub>3</sub> and H<sub>2</sub>SO<sub>4</sub> or HNO<sub>3</sub>  
369 (Pichford et al., 2009).

370 PC2 has high loadings of Na<sup>+</sup>, Mg<sup>2+</sup>, Cl<sup>-</sup>, and K<sup>+</sup> and moderate loadings of  
371 Ca<sup>2+</sup>. Those compounds indicate marine aerosols (Huang et al., 1999). The moderate  
372 loading of NO<sub>3</sub><sup>-</sup> is likely due to the reaction of HNO<sub>3</sub> and sea salt (Pakkanen, 1996).  
373 As in the PMF factor interpretation, the identification of component Sea Salt is  
374 relevant because the monitoring site is near the Atlantic.

375 PC3 has positive loadings of GEM, GOM, PBM and O<sub>3</sub>. The positive loadings on  
376 O<sub>3</sub> and GOM indicate the photochemical production of GOM (Huang et al., 2010).  
377 The positive loading of GEM is somewhat unexpected because the photochemical  
378 production of GOM consumes GEM thus leading to opposite signs of GEM and GOM  
379 (e.g. Huang et al., 2010). However, daily average concentrations were used in this



380 study instead of two-hour means in Huang et al. (2010). The daily GEM and GOM  
381 were indeed positively correlated ( $r=0.37$  in 2009, Table S2;  $0.31$  in 2010, Table S3).  
382 Using the same dataset, Cheng et al. (2013) conducted further analysis on  $O_3$   
383 concentrations and %GOM/TGM (TGM=GEM+GOM) ratios. The ratio is indicative  
384 of the degree of oxidation. The results showed that the %GOM/TGM ratio increased  
385 with  $O_3$  when  $O_3$  concentrations were greater than 40 ppb, suggesting gas phase  
386 oxidation of Hg at this coastal site. Therefore, this factor was named Photochemical  
387 Production of GOM.

388 PC4 represents Gas-particle Partitioning of Hg. The negative loading of PBM and  
389 the positive loading of GOM indicate the partition process. The positive loadings of  
390  $Ca^{2+}$  and  $K^+$  suggest soil aerosols (Cheng et al., 2012) which could be abundant at the  
391 Kejimikujik National Park.

392 Three out of four components (Combustion/industrial Emission, Photochemical  
393 Production of GOM and Gas-particle Partitioning of Hg) have significant association  
394 with ambient Hg concentrations at the site, while Sea Salt has little.

#### 395 ***Case 09-C&M***

396 Five principal components are extracted when meteorological data were included  
397 in PCA (Case 09-C&M, Table 7). The loadings in PC1-PC4 are similar with the  
398 loadings of PC1, PC2, PC4, PC3 in Case 09-C, respectively. Thus the names of those  
399 four components were retained. The inclusion of meteorological parameters resulted  
400 in small loadings of relative humidity ( $-0.26$ ) in PC1 and wind speed ( $0.32$ ) in PC2, as  
401 well as a moderate loading of wind speed ( $0.52$ ) in PC4. A large loading of  
402 temperature ( $0.94$ ) was observed in PC3. The opposite signs of temperature and PBM  
403 are consistent with the gas-particle partitioning process because low temperatures  
404 favor the formation of PBM (Rutter and Schauer, 2007). The lack of GEM in PC3  
405 (Case 09-C&M) did not affect the identification of this factor, because the partitioning  
406 of GEM onto particles is much weaker than that of GOM (Liu et al., 2007).

407 PC5 was derived mostly from meteorological variables. The negative loading of  
408 GOM and positive loadings of relative humidity and precipitation suggest removal of  
409 GOM by dew, cloud and precipitation (Cheng et al., 2013). The loading of GOM is  
410 small, nonetheless consistent with the wet deposition process because GOM is more  
411 easily removed compared to GEM due to its higher water solubility (Gaffney and



412 Marley, 2014). Therefore, this component was named Hg Wet Deposition.

413 Similar to Case 09-C, all components except Sea Salt are associated with ambient  
414 Hg concentrations. After the inclusion of meteorological data, each factor contains at  
415 least one meteorological parameter. The presence of meteorological variables did not  
416 contribute to the determination of the components except a new component Hg wet  
417 deposition was identified.

#### 418 *Case 10-C*

419 The component loadings of Case 10-C are listed in Table 8. PC1 was named  
420 Combustion Emission. The positive loadings of  $\text{HNO}_3$ ,  $\text{NO}_3^-$  and  $\text{SO}_4^{2-}$  are indicative  
421 of transport of combustion emission because their precursors ( $\text{NO}_2$  and  $\text{SO}_2$ ) are  
422 mainly released by combustion emissions (Liu et al., 2007). The high positive loading  
423 of  $\text{NH}_4^+$  represents transport of agriculture emissions of ammonia which may react  
424 with  $\text{H}_2\text{SO}_4$  and  $\text{HNO}_3$  during the transport process (Pitchford et al., 2009). The  
425 positive loadings of  $\text{Ca}^{2+}$  and  $\text{K}^+$  indicates biomass burning from wildfires or  
426 biomass-fueled power station (Andersen et al., 2007).

427 PC2 was named Sea Salt due to high loadings of  $\text{Na}^+$ ,  $\text{Mg}^{2+}$ , and  $\text{Cl}^-$ , because  
428 these three compounds are rich in sea water (Huang et al., 1999). PC3 has the same  
429 major variables as the component Photochemical Production of GOM in 2009.  
430 Therefore, PC3 was also named as such.

431 PC4 was assigned to Industrial Source. The positive loadings of GOM and  $\text{SO}_2$   
432 indicate coal combustion (Lynam and Keeler, 2006), although no combustion facilities  
433 were reported near the KEJ site in 2010 (Table S1). The positive loadings of  $\text{SO}_4^{2-}$  and  
434  $\text{HNO}_3$  are consistent with the transport of industrial emissions which release their  
435 precursors,  $\text{SO}_2$  and  $\text{NO}_x$  (Liu et al., 2007). Therefore, this factor was named  
436 Industrial Source. Two out of four factors (i.e. Photochemical Production of GOM and  
437 Industrial source) have significant association with Hg compounds.

#### 438 *Case 10-C&M*

439 As shown in Table 8, five principal components are extracted in Case 10-C&M.  
440 The loadings in PC1-PC3 and PC5 are similar with the loadings of PC1-PC4 in Case  
441 10-C, respectively. Thus the name of those four components were retained. PC4 in  
442 Case 10-C&M was named Hg Wet Deposition due to negative loadings of GOM and  
443 PBM and positive loadings of relative humidity, wind speed and precipitation, similar



444 with PC5 in Case 09-C&M (Table 7). Three out of five components (i.e.  
445 Photochemical Production of GOM, Industrial Source, and Hg Wet Deposition) were  
446 associated with Hg concentrations. The influence of meteorological data on  
447 identification of components were also similar to in 2009.

#### 448 *Comparison between PCA in year 2009 and 2010*

449 In each year, four components were extracted in PCA with air pollutants only.  
450 The two common factors between the two years are Photochemical Production of  
451 GOM and Sea Salt. The former has a strong association with Hg compounds, while  
452 the latter has little. Component Gas-particle Partitioning of Hg was only identified in  
453 2009, likely due to a lower percentage of PBM readings <MDL than those in 2010  
454 (Table 9, Case 2009 and 2010). It is also consistent with strong correlations between  
455 temperature as well as GOM and PBM ( $r=0.46$  and  $-0.43$ , Table S2) in 2009 but  
456 non-significant or weak correlations ( $r=-0.04$ , and  $-0.16$ , Table S3) in 2010.

457 The component Combustion/industrial Emission in 2009 affected PBM and SO<sub>2</sub>  
458 levels. It was split into two components in 2010, Combustion Emission and Industrial  
459 Source. The former was no longer strongly associated with any of the three Hg forms,  
460 while the latter was associated with GOM and SO<sub>2</sub>. This is probably due to the  
461 reduction of coal combustion in Canada and the USA, evident by lower provincial Hg  
462 (reduction of 39%) and SO<sub>2</sub> emissions (-35%) in 2010 (Table S1). The reductions in  
463 GEM, GOM, and SO<sub>2</sub> concentrations at the KEJ site were 3%, 75%, and 43%  
464 respectively in 2010 (Tables 1-2). The shifting of PBM & SO<sub>2</sub> relation in 2009 to  
465 GOM & SO<sub>2</sub> in 2010 is sustained by a strong correlation between PBM and SO<sub>2</sub>  
466 ( $r=0.63$ , Table S2) in 2009, but little correlation ( $r=0.06$ ) accompanied by a moderate  
467 correlation between GOM and SO<sub>2</sub> ( $r=0.30$ ) (Table S3) in 2010. The shift is also  
468 consistent with the PMF results where Industrial Sulfur accounted for 21% of PBM in  
469 2009 (Table S4) but 29% of GOM in 2010 (Table S5).

470 In both years, inclusion of meteorological parameters did not affect the  
471 identification of the four factors from air concentrations. However, relative humidity  
472 and precipitation yielded an additional component named Hg Wet Deposition.

473 Overall, the PCA results were largely consistent between the two years, in terms  
474 of the number of components, impact of meteorological parameters, and major  
475 processes associated with ambient Hg. The changing emissions/concentrations and the





476 resultant correlations among monitored air pollutants from one year to another are  
477 reflected in the limited shifting of variable loadings.

478

### 479 **3.3 Comparison of PMF and PCA results**

480 The PCA loadings and the factor profiles as well as factor contributions in PMF  
481 model have very different meanings. In PCA, variables with large loading indicate  
482 their correlation or association with that component derived from all samples. In PMF,  
483 presence of variables in profiles indicates their contribution to that source/process  
484 derived from all samples, while the contribution values are further quantified in  
485 source contribution tables of each sample. Therefore, a direct comparison between the  
486 PMF and PCA results is not feasible. However, the similarities and differences in the  
487 major sources/processes identified by each approach, chemical markers in each factor  
488 profile or component, and the impact/association of factors/components on Hg could  
489 reveal strength and weakness of each method.

490 A comparison of Table 5 and Tables 7-8 (cases with air concentrations only)  
491 shows that  $\text{Na}^+$ ,  $\text{Cl}^-$ , and  $\text{Mg}^{2+}$  are markers of Sea Salt in both PMF and PCA.  
492 Similarly, GEM, GOM, PBM and  $\text{O}_3$  indicate Photochemistry. Both methods suggest  
493 strong contribution to or association between Hg compounds and photochemistry, but  
494 weak with Sea Salt. Both methods identified combustion and industrial sources, while  
495 the variables in factors/components differed to some extent. Furthermore, combustion  
496 and industrial were separate sources in PMF in both years and in PCA in 2010, but  
497 combined as one component in PCA in 2009. Overall, PMF profiles are more  
498 consistent between the two years, while the PCA loadings are more sensitive to  
499 correlation among variables. However, the shift of PBM &  $\text{SO}_2$  to GOM &  $\text{SO}_2$   
500 loadings in PCA between the two years is consistent with the shift of those two pairs  
501 in Combustion & Industrial Sulfur profiles/contributions in PMF. On the other hand,  
502 Gas-particle Partitioning of Hg was only recognized in PCA. This is because the  
503 identification of this factor relies on negative association between PBM and GOM  
504 (Table 7), but such association is not reflected in PMF due to its non-negative nature.  
505 This is one of the limitations of PMF. Furthermore, the inclusion of meteorological  
506 conditions in PCA enables identification of a new component related with weather  
507 conditions. The good agreement between PMF and PCA outputs is consistent with a



508 comparison of receptor models in PM source appointment (Viana et al., 2007). A  
509 common weakness of PCA and PMF is the suggestiveness of factors/components.  
510 Other techniques, such as back trajectories, have been used in previous studies to  
511 verify some factors (Cheng et al. 2015). Overall, when accompanied by model  
512 performance evaluation, PMF results are with more confidence.

513

### 514 **3.4 Sensitivity of PMF results to data treatment**

#### 515 **3.4.1 Year 2009**

##### 516 ***Case 09+mean & Case 09+median***

517 The factor profiles of the six PMF cases in 2009 are displayed in Figure 1. In  
518 Case 09+mean and Case 09+median, all four factors have similar profiles as in Case  
519 2009. Compare with the base case, factor 3 (Photochemistry and Re-emission of Hg)  
520 has a higher contribution by  $\text{NO}_3^-$ , however it is common to observe  $\text{NO}_3^-$  from soil  
521 emissions (Parmar et al., 2001). GOM has a much smaller contribution in factor 1  
522 (Combustion Emission) (Figure 1, Table S4). This is likely because the correlation  
523 coefficients between GOM,  $\text{NH}_4^+$  and  $\text{SO}_4^{2-}$  become insignificant after imputation  
524 (Table S6). Consequently, GOM is not strongly related to that factor which is  
525 dominated by  $\text{NH}_4^+$  and  $\text{SO}_4^{2-}$ . Changing correlation among variables is a  
526 shortcoming of imputation (Huang et al., 1999).

527

##### 528 ***Case 09+RM & Case 09-RM***

529 As shown in Figure 1 and Table S4, by combining GOM and PBM into RM,  
530 RM replaced PBM instead of GOM in related factors as major variables with similar  
531 contributions. This is because the median concentration of PBM is approximately 5  
532 time of the median concentration of GOM (Table 9). Once these two forms are  
533 combined to RM, the variance of RM is dominated by PBM. The presence of other  
534 compounds including GEM in factor profiles/contributions in these two cases are  
535 similar to those in Case 2009.

##### 536 ***Case 09ScaleRM***

537 The factor profiles were similar to those in Case 2009 (Figure 1). The same can  
538 be said about factor contributions to speciated Hg (Table S4).



539 ***Performance***

540 Case 09-RM, Case 09+RM and Case 09ScaleRM have similar performances with  
541 Case 2009, on distribution of scaled residuals (Table 6). Imputation (Case 09+mean  
542 and Case 09-median) worsened the performance because the scaled residuals are  
543 concentrated near zero for gaseous Hg.

544 In terms of the coefficients of determination ( $R^2$ ) and the slopes of the regression  
545 line for speciated Hg in Obs/Pred scatter plot (Table 6, Figure S1), imputation (Case  
546 09+mean and Case 09+median) deteriorated PMF performance compared to the base  
547 case. This is not unexpected because the use of a constant imputation value reduced  
548 the variance in observed concentrations (Table 9). The similar performances on GEM  
549 in Case 2009, Case 09+RM, Case 09-RM, and Case 09ScaleRM indicate combining,  
550 excluding, or scaling GOM and PBM, respectively, did not affect the performance on  
551 GEM. The performances on RM are similar to that of PBM in Case 2009 because the  
552 RM concentrations are dominated by PBM. Using scaling factors to increase GOM  
553 and PBM concentrations resulted in better performances on those two forms than in  
554 the base case. This is attributable to a significant reduction in percent of  
555 concentrations below MDL (Table 9).

556 The changes in model performance are more evident in the observed and  
557 predicted time series (Figure S3). Compared with the base case, imputation led to  
558 more fluctuation in the predicted GEM values, thus slightly worse. RM had better  
559 model-measurement agreement than GOM or PBM as individual compound. The  
560 agreement was also improved by scaling GOM or PBM. The peak values (PBM in  
561 period 1 and both forms in period 2) were better reproduced and the over prediction in  
562 period 3 with low concentrations was greatly corrected.

563 Compared with the base case, the distributions of the ratios of predicted to  
564 observed Hg concentrations and the ratio of predicted to observe annual means  
565 changed little for GEM among the six cases (Figure 3, Table S4). Scaling GOM and  
566 PBM improved model-measurement agreement of those two forms, evident by a  
567 much narrower range and a shift toward smaller values in the distribution of ratios.

568 **3.4.2 Year 2010**



569 ***Case 10+mean & Case 10+median***

570 Factor profiles (Figure 2) and contributions (Table S5) after imputation have  
571 minor changes compared to those in Case 2010. However, less changes were observed  
572 with the use of median imputation. The small deviations after imputations is probably  
573 because only a small fraction (4%) of Hg concentrations were missing in 2010 than in  
574 2009 (31-41%). Although HNO<sub>3</sub>, SO<sub>2</sub>, and inorganic ions have up to 19% missing  
575 values (Table 2), the correlations between each of the three Hg forms and other  
576 compounds changed little (Table S7).

577 ***Case 10+RM & Case 10-RM***

578 The impact of combining or removing GOM and PBM (Figure 2, Table S5) is the  
579 same as in 2009. The dominance of PBM in RM is stronger in 2010 with the ratio of  
580 median PBM to median GOM concentration being approximately 10 (Table 9).

581 Overall, excluding or combining GOM and PBM did not affect the source  
582 identification in PMF model in both years (Figures 1 and 2). However, the  
583 identification of the factors relying on GOM or PBM only (e.g. gas-particle  
584 partitioning of Hg) may be affected after combining or excluding GOM and PBM.  
585 In this study, such factors were not encountered in PMF. Nonetheless, excluding or  
586 combining GOM and PBM did affect the source contributions. After combining GOM  
587 and PBM, factors contributing to GOM only (Combustion Emission, 2009; Industrial  
588 Sulfur, 2010, Table 10) did not contribute to any Hg forms, and the factor contributing  
589 to PBM only (Industrial Sulfur, 2009) was contributing to RM, due to dominance of  
590 PBM in RM. In both years, using three Hg forms instead of GEM only led to more Hg  
591 sources/processes identified. Therefore, monitoring speciated Hg could help us better  
592 understand Hg cycling.

593 ***Case 10ScaleRM***

594 The factor profiles and contributions of Case 10ScaleRM are similar to those in  
595 Case 2010 (Figure 2, Table S5). A noticeable deviation is the much smaller  
596 contribution by GOM in factor 2 compared to Case 2010. However, factor 2 was still  
597 assigned to Industrial Sulfur because of the presence of SO<sub>2</sub> and NO<sub>3</sub><sup>-</sup>.

598 ***Performance***



599 Firstly, the distribution of scaled residuals as well as  $R^2$  value and the slope of the  
600 regression line for speciated Hg in Obs/Pred scatter plot was evaluated for the six  
601 cases (Table 6, Figure S2). Similar to 2009, the comparable performances observed in  
602 Case 2010, Case 10-RM, Case 10+RM, and Case 10ScaleRM indicate that the model  
603 performance on GEM is insensitive to excluding, scaling, or combining GOM and  
604 PBM to RM. Case 10ScaleRM also has the best performances on GOM and PBM  
605 among all the cases in 2010. Unlike in 2009, the negative impact of imputation was  
606 smaller when median value was used, compared with the mean imputation.

607 Secondly, in the observed and predicted time series (Figure S4), imputation  
608 resulted in more severe fluctuation in predicted GEM concentration as in 2009, but  
609 less so when median values were used. Scaling of GOM or PBM also improved the  
610 reproducibility of day-to-day variability in the observed values, owing to a large  
611 reduction in concentrations below MDL (Table 9). Among the 6 cases, the most  
612 significant change is in PBM with imputation. There were additional high  
613 concentration episodes in early 2010 when imputation of non-Hg compounds brought  
614 back Hg concentrations otherwise removed by listwise deletion in the base case,  
615 leading to increased standard deviation (Table 9). Those peaks were completely  
616 missed by the model, leading to deteriorated agreement.

617 Finally, the distributions of the ratios of predicted to observe Hg concentrations  
618 and the ratio of predicted to observe annual means changed little among the first five  
619 cases in 2010 (Figure 3 and Table S5). The exceptions are under prediction of the  
620 annual mean of PBM in the two imputation cases and over prediction for RM.  
621 Compared with the base case, the distribution of ratios for GOM and PBM became  
622 narrower and shifted toward smaller values, but leading to under prediction of PBM.

### 623 3.4.3 Comparison of 2009 and 2010 among different data treatments

624 The different characteristics of Hg forms led to different impact of data treatment  
625 on model results and performances in the two years. Imputation using geometric  
626 mean and median values led to minor changes in factor profiles in both years, with  
627 more variations in contributions of Hg forms in 2009 but non-mercury compounds in  
628 2010. This is likely because the Hg and non-Hg compounds were missing at a larger  
629 percentage in 2009 and 2010, respectively. The lack of significant impact is likely due



630 to already high sample to compound ratios (161 samples/15 compounds in 2009, 290  
631 samples/14 compounds in 2010, Tables 1-3). Huang et al. (1999) have reported that  
632 mean imputation generally yielded better PMF results than listwise deletion,  
633 especially with higher percentage of missing values. Particularly, composition of  
634 crustal and marine factors were closer to those of crust and sea water. Imputation  
635 resulted in degraded performance on all three Hg forms, but for different reasons. For  
636 GEM, it is largely due to more fluctuation than the already over predicted one in the  
637 base case in both years. For PBM in 2010, the peak values otherwise removed in  
638 listwise deletion (base case) are beyond the model's ability to match. This seems to be  
639 a random occurrence and is an uncertainty of imputation. Between geometric mean  
640 and median imputations, the impact was similar in both years for each of the three Hg  
641 forms. The exception is with median imputation in 2010, there was less deviation in  
642 factor profile/contribution from the base case. The reason is unclear because the  
643 difference in geometric mean and median was very small for GEM in both years and  
644 slightly greater in 2009 for GOM and PBM (Tables 1-2).

645 In both years, some changes in the factor profiles and factor contributions but  
646 little changes in model performances were observed in the cases excluding GOM and  
647 PBM. Scaling GOM and PBM or combining them into RM improved  
648 model-measurement agreement, suggesting the approach is effective in both year in  
649 spite of large percentages of below MDL values (GOM, 78% in 2009 vs. 96% in 2010;  
650 PBM, 48% in 2009 vs. 46% in 2010, Tables 1-2). The improvement is largely  
651 attributable to reduction in concentrations below MDL (Table 9) which in turn  
652 reduced PMF uncertainty expressed in equation (2). Another benefit of using a  
653 variable scaling factor is reduced data variability as indicated by smaller coefficients  
654 of variation in Table 9. PMF is more likely reproducing well compounds with less  
655 variability. However, there is little evidence that the scientific uncertainties of scaled  
656 GOM and PBM concentrations are indeed reduced from that of the original dataset.

657



658 **4. Conclusions**

659 Source apportionment analysis was conducted with PMF and PCA using  
660 concentrations of speciated Hg and other air pollutants collected at KEJ site in 2009  
661 and 2010. Year 2010 was characterized by reduced Hg and SO<sub>2</sub> emissions compared  
662 with 2009. However, GOM is more sensitive to the decrease in Hg emissions while  
663 GEM and PBM are not, underscoring the benefits of speciated Hg measurements. It  
664 was found that consideration of emission inventories and correlation among air  
665 pollutants is useful in factor/component interpretation.

666 Using PMF, the nature of each of the four factors identified was the same in 2009  
667 and 2010. In both years, ambient concentration of all three Hg forms at the KEJ site  
668 were dominated by contributions from factor Photochemistry and Re-emission, and  
669 the contribution by Sea Salt was the smallest. However, slight variations between the  
670 two years were observed in the contributions by the other two factors (Combustion  
671 Emission, Industrial Sulfur).

672 Good agreement was found between PMF and PCA results. In each year, four  
673 components were extracted in PCA with air pollutants only. Three or four of them  
674 overlapped with factors obtained in PMF. PCA results suggest little association  
675 between Hg and Sea Salt, consistent with PMF. Furthermore, PMF and PCA had  
676 similar shift of source profile/contribution from one year to another, suggesting both  
677 methods were able to respond to changing concentration levels, and interrelationships  
678 among the air pollutants. In both years, inclusion of meteorological parameters in  
679 PCA led to extraction of an additional component Hg Wet Deposition while the  
680 identification of other components was not affected. Therefore, PCA is superb to PMF  
681 in terms of identifying factors related to atmospheric processes. With regards to  
682 atmospheric processes represented by negative correlation among variables, such as  
683 Gas-particle Partitioning of Hg (Table 8), PCA is more likely to identify them because  
684 component loadings reflect correlations, while it is difficult for PMF because its  
685 variable contributions in source profile are all positive.

686 A comprehensive PMF model performance evaluation was conducted for each of  
687 the three Hg forms. Between the two years, the model performance was comparable.  
688 In both years, the observed daily GEM concentrations were well reproduced, but



689 relatively poor for GOM and PBM. On an annual basis, the model-measurement  
690 agreement of annual mean concentrations were excellent for GEM, very good for  
691 PBM and acceptable for GOM.

692 The sensitivity of PMF results and model performance to different approaches of  
693 dealing with missing values and concentrations with large uncertainties was  
694 investigated. In our study of more than 160 samples with 15 or 14 air pollutants,  
695 increasing the sample size by geometric mean or median imputation of missing values  
696 is not effective in improving the model performance. With over 70% GOM and over  
697 40% PBM concentrations below MDL in our dataset, the impact of large measurement  
698 uncertainties in GOM and PBM is much more significant. Scaling GOM and PBM to  
699 increase their concentrations or combining them to reactive mercury is effective in  
700 improving the model-measurement agreement. The identification of sources/processes  
701 and their contributions to speciated Hg are relatively insensitive to any of the data  
702 treatment options considered. The exception is that less sources/processes affecting  
703 ambient Hg were identified when GOM and PBM were excluded, further underlining  
704 the importance of monitoring speciated Hg.

705 The good agreement between PCA and PMF results in both years is encouraging  
706 although these two methods bear little resemblance. PMF partitions observed  
707 concentrations by solving mass balance equations, while PCA is a data reduction tool  
708 to explain majority of variances in the entire dataset with a small number of  
709 components. Our observation was made possible by the use of multiple-year dataset.  
710 Future studies should conduct more PMF and PCA comparisons to validate our  
711 findings.

712 Overall, PMF results are quantitative and with more confidence with model  
713 performance evaluation. However, when ancillary air pollutant data are available, it is  
714 recommended to carry out both PCA and PMF simulations to verify the  
715 sources/processes identified.

716 Our PMF results suggest that PMF has difficulties reproducing daily  
717 concentrations of GOM and PBM, because of high concentration episodes and large  
718 uncertainties due to low concentrations and large percentage of below MDL values.  
719 More attention should be devoted to those issues in future studies.





720

721 **Acknowledgements:** Funding of this project was provided by Environment Canada  
722 and National Sciences and Engineering Research Council of Canada. The authors  
723 acknowledge John Dalziel and Rob Tordon of Environment Canada for providing  
724 mercury data and US EPA for the PMF model used in this study.

725

726 **References**

727 Andersen, Z. J., Wahlin, P., Raaschou-Nielsen, O., Scheike, T., and Loft, S.: Ambient  
728 particle source apportionment and daily hospital admissions among children  
729 and elderly in Copenhagen, *Journal of Exposure Science and Environmental  
730 Epidemiology*, 17, 625-636, 10.1038/sj.jes.7500546, 2007.

731 Carpi, A.: Mercury from combustion sources: a review of the chemical species  
732 emitted and their transport in the atmosphere, *Water, Air, Soil Pollut.*, 98,  
733 241-254, 10.1023/A:1026429911010, 1997.

734 Croghan, C. W., and Egeghy, P. P.: Methods of dealing with values below the limit of  
735 detection using SAS, available at:  
736 <http://analytics.ncsu.edu/sesug/2003/SD08-Croghan.pdf> (last access: May 30,  
737 2016), 2003.

738 Cheng, I., Lu, J., and Song, X.: Studies of potential sources that contributed to  
739 atmospheric mercury in Toronto, Canada., *Atmos. Environ.*, 43, 6145-6158,  
740 10.1016/j.atmosenv.2009.09.008, 2009.

741 Cheng, I., Zhang, L., Blanchard, P., Graydon, J. A., and Louis, V. L. S.:  
742 Source-receptor relationships for speciated atmospheric mercury at the  
743 Remote Experimental Lakes Area, Northwestern Ontario, Canada, *Atmos.  
744 Chem. Phys.*, 12, 1903-1922, 10.5194/acp-12-1903-2012, 2012.

745 Cheng, I., Zhang, L., Blanchard, P., Dalziel, J., Tordon, R., Huang, J., and Holsen, T.  
746 M.: Comparisons of mercury sources and atmospheric mercury processes  
747 between a coastal and inland site, *J. Geophys. Res-Atmos.*, 118, 2434-2443,  
748 10.1002/jgrd.50169, 2013.

749 Cheng, I., Xu, X., and Zhang, L.: Overview of receptor-based source apportionment  
750 studies for speciated atmospheric mercury, *Atmos. Chem. Phys.*, 15,  
751 7877-7895, 10.5194/acp-15-7877-2015, 2015.

752 Cheng, I., Zhang, L., and Xu, X.: Impact of measurement uncertainties on receptor  
753 modeling of speciated atmospheric mercury, *Scientific Reports*, 6, 20676,  
754 10.1038/srep20676, 2016.

755 Environment Canada (EC): National Pollutants Release Inventory (NPRI) Datasets,  
756 available at:  
757 <https://www.ec.gc.ca/inrp-npri/default.asp?lang=en&n=0EC58C98-1> (last  
758 access: May 29, 2016), 2016.

759 Evers, D. C., Han, Y.-J., Driscoll, C. T., Kamman, N. C., Goodale, M. W., Lambert,  
760 K. F., Holsen, T. M., Chen, C. Y., Clair, T. A., and Butler, T.: Biological  
761 mercury hotspots in the Northeastern United States and Southeastern Canada,  
762 *BioScience*, 57, 29-43, 10.1641/B570107, 2007.



- 763 Gaffney, J. S., and Marley, N. A.: In-depth review of atmospheric mercury: sources,  
764 transformations, and potential sinks, *Energy and Emission Control*  
765 *Technologies*, 2, 1-21, 10.2147/EECT.S37038, 2014.
- 766 Goodsite, M. E., Plane, J. M. C., and Skov, H.: A theoretical study of the oxidation of  
767 Hg<sup>0</sup> to HgBr<sub>2</sub> in the troposphere, *Environ. Sci. Technol.*, 38, 1772-1776,  
768 10.1021/es034680s, 2004.
- 769 Gustin, M. S., Lindberg, S. E., and Weisberg, P.J.: An update on the natural sources  
770 and sinks of atmospheric mercury, *Applied Geochemistry*, 23, 482-493, 2008.
- 771 Gustin, M. S., Amos, H. M., Huang, J., Miller, M. B., & Heidecorn, K.: Measuring  
772 and modeling mercury in the atmosphere: a critical review, *Atmos. Chem.*  
773 *Phys.*, 15(10), 5697-5713. 10.5194/acp-15-5697-2015, 2015.
- 774 Hedberg, E., Gidhagen, L., and Johansson, C.: Source contributions to PM<sub>10</sub> and  
775 arsenic concentrations in Central Chile using positive matrix factorization,  
776 *Atmos. Environ.*, 39, 549-561, 10.1016/j.atmosenv.2004.11.001, 2005.
- 777 Henry, R. C.: Multivariate receptor models, in: *Receptor modeling for air quality*  
778 *management*, 1st ed., edited by: Hopke, P. K., Elsevier Science Publishers,  
779 Amsterdam, 1991.
- 780 Holmes, C. D., Jacob, D. J., Mason, R. P., & Jaffe, D. A.: Sources and deposition of  
781 reactive gaseous mercury in the marine atmosphere. *Atmos. Environ.*, 43(14),  
782 2278-2285, 10.1016/j.atmosenv.2009.01.051, 2009.
- 783 Hopke, P. K.: Review of receptor modeling methods for source apportionment, *J. Air.*  
784 *Waste. Manage.*, 66, 237-259, 10.1080/10962247.2016.1140693, 2016.
- 785 Huang, S., Rahn, K. A., and Arimoto, R.: Testing and optimizing two factor-analysis  
786 techniques on aerosol at Narragansett, Rhode Island, *Atmos. Environ.*, 33,  
787 2169-2185, 10.1016/S1352-2310(98)00324-0, 1999.
- 788 Huang, J., Choi, H.-D., Hopke, P. K., and Holsen, T. M.: Ambient Hg sources in  
789 Rochester, NY: results from principle components analysis (PCA) of Hg  
790 monitoring network data, *Environ. Sci. Technol.*, 44, 8441-8445,  
791 10.1021/es102744j, 2010.
- 792 Kaiser, H. F.: *The Application of Electronic Computers to Factor Analysis*, *Educ.*  
793 *Psychol. Meas.*, 20, 141-151, 10.1177/001316446002000116, 1960.
- 794 Lee, E., Chan, C. K., & Paatero, P.: Application of positive matrix factorization in  
795 source apportionment of particulate pollutants in Hong Kong. *Atmos. Environ.*,  
796 33(19), 3201-3212, 10.1016/S1352-2310(99)00113-2, 1999.
- 797 Liu, B., Keeler, G. J., Dvonch, J. T., Barres, J. A., Lynam, M. M., Marsik, F. J., and  
798 Morgan, J. T.: Temporal variability of mercury speciation in urban air, *Atmos.*  
799 *Environ.*, 41, 1911-1923, 10.1016/j.atmosenv.2006.10.063, 2007.
- 800 Lynam, M. M., and Keeler, G. J.: Artifacts associated with the measurement of  
801 particulate mercury in an urban environment: the influence of elevated ozone  
802 concentrations, *Atmos. Environ.*, 39, 3081-3088,  
803 10.1016/j.atmosenv.2005.01.036, 2005.
- 804 Lynam, M. M., and Keeler, G. J.: Source-receptor relationships for atmospheric  
805 mercury in urban Detroit, Michigan, *Atmos. Environ.*, 40, 3144-3155,  
806 10.1016/j.atmosenv.2006.01.026, 2006.
- 807 Obrist, D., Tas, E., Peleg, M., Matveev, V., Fäin, X., Asaf, D., and Luria, M.:  
808 Bromine-induced oxidation of mercury in the mid-latitude atmosphere, *Nat.*  
809 *Geosci.*, 4, 22-26, 10.1038/ngeo1018, 2011.



- 810 Pakkanen, T. A.: Study of formation of coarse particle nitrate aerosol, Atmos.  
811 Environ., 30, 2475-2482, 10.1016/1352-2310(95)00492-0, 1996.
- 812 Pal, B., and Ariya, P. A.: Studies of ozone initiated reactions of gaseous mercury:  
813 kinetics, product studies, and atmospheric implications, Phys. Chem. Chem.  
814 Phys., 6, 572-579, 10.1039/B311150D, 2004.
- 815 Parmar, R. S., Satsangi, G. S., Kumari, M., Lakhani, A., Srivastava, S. S., and Prakash,  
816 S.: Study of size distribution of atmospheric aerosol at Agra, Atmos. Environ.,  
817 35, 693-702, 10.1016/S1352-2310(00)00317-4, 2001.
- 818 Pavlovic, R. T., Nopmongcol, U., Kimura, Y., and Allen, D. T.: Ammonia emissions,  
819 concentrations and implications for particulate matter formation in Houston,  
820 TX, Atmos. Environ., 40, 538-551, 10.1016/j.atmosenv.2006.04.071, 2006.
- 821 Pekey, H., Karakaş, D., & Bakoglu, M.: Source apportionment of trace metals in  
822 surface waters of a polluted stream using multivariate statistical analyses.  
823 Marine Pollution Bulletin, 49(9), 809-818, 2004.
- 824 Pirrone, N., Cinnirella, S., Feng, X., Finkelman, R.B., Friedli, H.R., Leaner, J., Mason,  
825 R., (...), Telmer, K.: Global mercury emissions to the atmosphere from  
826 anthropogenic and natural sources. Atmos. Chem. Phys., 10, 5951-5964,  
827 2010.
- 828 Pitchford, M. L., Poirot, R. L., Schichtel, B. A., and Malm, W. C.: Characterization of  
829 the winter midwestern particulate nitrate bulge, J. Air Waste Manage., 59,  
830 1061-1069, 10.3155/1047-3289.59.9.1061, 2009.
- 831 Polissar, A. V., Hopke, P. K., Paatero, P., Malm, W. C., and Sisler, J. F.: Atmospheric  
832 aerosol over Alaska: 2. Elemental composition and sources, J. Geophys.  
833 Res-Atmos., 103, 19045-19057, 10.1029/98JD01212, 1998.
- 834 Rutter, A. P., and Schauer, J. J.: The effect of temperature on the gas-particle  
835 partitioning of reactive mercury in atmospheric aerosols, Atmos. Environ., 41,  
836 8647-8657, 10.1016/j.atmosenv.2007.07.024, 2007.
- 837 Tekran Inc.: Products. Ambient Air, available at:  
838 <http://www.tekran.com/products/ambient-air/overview/> (last access: May 29,  
839 2016), 2010.
- 840 United Nations Environmental Programme (UNEP): Global Mercury Assessment  
841 2013: Sources, Emissions, Releases and Environmental Transport. UNEP  
842 Chemicals Branch, Geneva, Switzerland, available at:  
843 <http://www.unep.org/PDF/PressReleases/GlobalMercuryAssessment2013.pdf>  
844 (last access: May 30, 2016), 2013.
- 845 US Environmental Protection Agency (US EPA): Clean Air Markets: 2010 Progress  
846 Report Emission, Compliance, and Market Analyses, available at:  
847 <https://www.epa.gov/airmarkets/acid-rain-program-historical-reports> (last  
848 access June 9, 2016), 2011
- 849 US Environmental Protection Agency (US EPA): EPA Positive Matrix Factorization  
850 (PMF) 5.0 Fundamentals and User Guide, available at:  
851 [https://www.epa.gov/sites/production/files/2015-02/documents/pmf\\_5.0\\_user\\_](https://www.epa.gov/sites/production/files/2015-02/documents/pmf_5.0_user_guide.pdf)  
852 [guide.pdf](https://www.epa.gov/sites/production/files/2015-02/documents/pmf_5.0_user_guide.pdf) (last access: May 30, 2016), 2014a.
- 853 US Environmental Protection Agency (US EPA): Positive Matrix Factorization  
854 Model (version 5.0), available at:  
855 [https://www.epa.gov/sites/production/files/2015-03/epa\\_pmf\\_5.0\\_setup.exe](https://www.epa.gov/sites/production/files/2015-03/epa_pmf_5.0_setup.exe)  
856 (last access: June 6, 2015), 2014b.



- 857 Viana, M., Pandolfi, M., Minguillón, M. C., Querol, X., Alastuey, A., Monfort, E.,  
858 and Celades, I.: Inter-comparison of receptor models for PM source  
859 apportionment: case study in an industrial area, *Atmos. Environ.*, 42,  
860 3820-3832, 10.1016/j.atmosenv.2007.12.056, 2008.
- 861 Wyn, B., Kidd, K. A., Burgess, N. M., Curry, R. A., and Munkittrick, K. R.:  
862 Increasing mercury in yellow perch at a hotspot in Atlantic Canada,  
863 Kejimikujik National Park, *Environ. Sci. Technol.*, 44, 9176-9181,  
864 10.1021/es1018114, 2010.
- 865 Zhang L., Vet R., Wiebe A., Mihele C., Sukloff B., Chan E., Moran M., and Iqbal S.:  
866 Characterization of the size-segregated water-soluble inorganic ions at eight  
867 Canadian rural sites, *Atmos. Chem. Phys.*, 8, 7133-7151, 2008.
- 868 Zhang L., Wang S., Wu Q., Wang F., Lin C.-J., Zhang L., Hui M., and Hao J.:  
869 Mercury transformation and speciation in flue gases from anthropogenic  
870 emission sources: A critical review, *Atmos. Chem. Phys.*, 16, 2417-2433,  
871 2016.  
872



873 **List of Tables**

874 Table 1. General statistics of air pollutant concentrations (in  $\mu\text{g}/\text{m}^3$  unless otherwise  
875 noted) in 2009.

876 Table 2. General statistics of air pollutant concentrations (in  $\mu\text{g}/\text{m}^3$  unless otherwise  
877 noted) in 2010, MDL same as in Table 1.

878 Table 3. PMF case design with different treatments of speciated Hg data.

879 Table 4. PCA input and set-up.

880 Table 5. Factor profiles (concentration  $>25\%$ , between 20% and 25% in parenthesis)  
881 of Case 2009 and Case 2010.

882 Table 6. PMF model performances on speciated mercury in 2009 and 2010.

883 Table 7. PCA component loadings ( $>0.25$ ) of Case 09-C and Case 09-C&M.

884 Table 8. PCA component loadings ( $>0.25$ ) of Case 10-C and Case 10-C&M.

885 Table 9. General statistics of speciated Hg with different data treatment options.

886 Table 10. Impact of combining or excluding GOM and PBM on PMF factor  
887 contributions ( $>15\%$ ) to Hg compounds.

888



889 **List of Figures**

890 Figure 1. PMF source profiles in percent of concentration, 2009.

891 Figure 2. PMF source profiles in percent of concentration, 2010.

892 Figure 3. Box plot of predicted to observed concentration ratios (upper whisker- upper  
893 25% of the distribution excluding outliers; interquartile range box - middle 50%  
894 of the data; horizontal line in the box - median; lower whisker- lower 25% of  
895 the distribution excluding outliers;  $\oplus$  - mean).

896


 Table 1. General statistics of air pollutant concentrations (in  $\mu\text{g}/\text{m}^3$  unless otherwise noted) in 2009.

Compound	Percent of missing values	Method detection limit (MDL)	Percent of values <MDL	Geometric Mean	Median	Mean	Standard deviation	Coefficient of variability (%)
GEM ( $\text{ng}/\text{m}^3$ )	31%	0.1	0%	1.37	1.41	1.39	0.26	18.7
GOM ( $\text{pg}/\text{m}^3$ )	32%	2	78%	0.57	0.42	1.77	3.70	209
PBM ( $\text{pg}/\text{m}^3$ )	41%	2	48%	1.78	2.15	2.81	2.72	96.8
PM	20%	1	9%	2.71	2.91	3.44	2.49	72.4
O <sub>3</sub>	0%	4.3	0%	59.4	62.1	62.4	19.1	30.6
SO <sub>2</sub>	3%	0.002	0%	0.20	0.22	0.40	0.51	128
HNO <sub>3</sub>	3%	0.05	12%	0.13	0.12	0.19	0.22	116
Ca <sup>2+</sup>	1%	0.002	0%	0.05	0.05	0.06	0.04	66.7
K <sup>+</sup>	1%	0.029	17%	0.04	0.03	0.04	0.03	75.0
Na <sup>+</sup>	1%	0.05	9%	0.25	0.30	0.43	0.47	109
Mg <sup>2+</sup>	1%	0.0004	2%	0.04	0.04	0.06	0.06	100
Cl <sup>-</sup>	1%	0.046	23%	0.19	0.23	0.46	0.64	139
NO <sub>3</sub> <sup>-</sup>	1%	0.06	9%	0.18	0.17	0.28	0.39	139
NH <sub>4</sub> <sup>+</sup>	1%	0.001	0%	0.19	0.17	0.28	0.32	114
SO <sub>4</sub> <sup>2-</sup>	1%	0.05	0%	0.78	0.76	1.14	1.27	111


 Table 2. General statistics of air pollutant concentrations (in  $\mu\text{g}/\text{m}^3$  unless otherwise noted) in 2010, MDL same as in Table 1.

Compound	Percent of missing values	Percent of values <MDL	Geometric Mean	Median	Mean	Standard deviation	Coefficient of variability (%)
GEM ( $\text{ng}/\text{m}^3$ )	4%	0%	1.34	1.38	1.35	0.17	12.6
GOM ( $\text{pg}/\text{m}^3$ )	4%	96%	0.27	0.21	0.44	0.64	145
PBM ( $\text{pg}/\text{m}^3$ )	4%	46%	2.08	2.20	3.40	4.13	121
O <sub>3</sub>	1%	0%	62.2	63.4	64.5	16.6	25.7
SO <sub>2</sub>	19%	1%	0.10	0.13	0.23	0.31	135
HNO <sub>3</sub>	19%	25%	0.10	0.10	0.18	0.22	122
Ca <sup>2+</sup>	19%	0%	0.04	0.04	0.07	0.13	186
K <sup>+</sup>	19%	46%	0.04	0.03	0.06	0.07	117
Na <sup>+</sup>	19%	16%	0.20	0.24	0.40	0.53	133
Mg <sup>2+</sup>	19%	0%	0.03	0.04	0.05	0.06	120
Cl <sup>-</sup>	19%	27%	0.14	0.15	0.46	0.83	180
NO <sub>3</sub> <sup>-</sup>	19%	21%	0.14	0.13	0.25	0.36	144
NH <sub>4</sub> <sup>+</sup>	19%	0%	0.16	0.15	0.30	0.57	190
SO <sub>4</sub> <sup>2-</sup>	19%	0%	0.69	0.64	1.11	1.65	149





Table 3. PMF case design with different treatments of speciated Hg data.

Case		Input variables	Treatment of missing value	Sample size	
2009	2010			2009	2010
2009 (base case)	2010 (base case)	All compounds	Excluding listwise	161	290
09+Mean	10+Mean	All compounds	Geometric mean imputation	365	365
09+Median	10+Median	All compounds	Median imputation	365	365
09+RM	10+RM	All compounds, but combining GOM & PBM to RM	Excluding listwise	161	290
09-RM	10-RM	All compounds, except GOM & PBM	Excluding listwise	201	290
09ScaleRM	10ScaleRM	All compounds, GOM & PBM scaled	Excluding listwise	161	290



Table 4. PCA input and set-up.

Case	Year	Input variables	Sample size	Other settings
09-C	2009	All compounds	161	1) Missing value: Listwise deletion
09-C&M	2009	All compounds and meteorological parameters	159	2) Components to keep: eigenvalues >1)
10-C	2010	All compounds	290	3) Rotation: Varimax
10-C&M	2010	All compounds and meteorological parameters	285	4) Cut-off value for major loadings: 0.25



Table 5. Factor profiles (concentration &gt;25%, between 20% and 25% in parenthesis) of Case 2009 and Case 2010.

Compound	2009				2010			
	F1	F2	F3	F4	F1	F2	F3	F4
GEM			76				79	
GOM	31		69			37	59	
PBM		29	63				81	
PM	42		34		-	-	-	-
O <sub>3</sub>			72				80	
SO <sub>2</sub>		82				93		
HNO <sub>3</sub>	54	(21)	(25)		64	26		
Ca <sup>2+</sup>	(19)		45	31		29	36	(21)
K <sup>+</sup>	(22)		37	39	51		27	(23)
Na <sup>+</sup>				86				83
Mg <sup>2+</sup>				83				75
Cl <sup>-</sup>				100				100
NO <sub>3</sub>	(25)	(23)		40		41	(23)	
NH <sub>4</sub> <sup>+</sup>	71				87			
SO <sub>4</sub> <sup>2-</sup>	64				79			
Factor	Combustion emission	Industrial sulfur	Photochemistry & re-emission of Hg	Sea salt	Combustion emission	Industrial sulfur	Photochemistry & re-emission of Hg	Sea salt



Table 6. PMF model performances on speciated mercury in 2009 and 2010.

Hg form	Case	Distribution	Number of scaled residuals greater than 3	Coefficient of determination ( $R^2$ )	Slope of regression line
GEM	09	Normal	0	0.28	0.59
	09+mean	Concentrated near zero	5	0.17	0.57
	09+median	Concentrated near zero	5	0.15	0.54
	09+RM	Normal	0	0.29	0.59
	09-RM	Normal	1	0.25	0.59
	09ScaleRM	Normal	0	0.28	0.58
	10	Normal	2	0.46	1.29
	10+mean	Normal	19	0.32	1.26
	10+median	Normal	2	0.41	1.26
	10+RM	Normal	2	0.46	1.31
	10-RM	Normal	2	0.47	1.31
	10ScaleRM	Normal	1	0.44	1.19
GOM	09	Right skewed	17	0.23	0.09
	09+mean	Concentrated near zero, right skewed	17	0.08	0.05
	09+median	Concentrated near zero, right skewed	19	0.09	0.05
	09+RM	-	-	-	-
	09-RM	-	-	-	-
	09ScaleRM	Right skewed	26	0.33	0.18
	10	Narrower	0	0.31	0.29
	10+mean	Narrower	0	0.23	0.22
	10+median	Narrower	0	0.28	0.28
	10+RM	-	-	-	-
	10-RM	-	-	-	-
	10ScaleRM	Narrower	0	0.42	0.33
PBM	09	Normal	5	0.57	0.39
	09+mean	Right skewed	6	0.33	0.32
	09+median	Right skewed	6	0.34	0.34
	09+RM	Right skewed (RM)	8 (RM)	0.48(RM)	0.31(RM)
	09-RM	-	-	-	-
	09ScaleRM	Left skewed	2	0.59	0.48
	10	Right skewed	14	0.13	0.09
	10+mean	Right skewed	28	0.15	0.09
	10+median	Right skewed	29	0.16	0.08
	10+RM	Right skewed (RM)	5	0.19	0.15
	10-RM	-	-	-	-
	10ScaleRM	Normal	18	0.25	0.24



Table 7. PCA component loadings (&gt;0.25) of Case 09-C and Case 09-C&amp;M.

Variable	Case 10-C				Case 10-C&M				
	PC1	PC2	PC3	PC4	PC1	PC2	PC3	PC4	PC5
GEM			0.86	0.27				0.80	
GOM			0.26	0.84			0.64	0.41	-0.29
PBM	0.63		0.50	-0.33	0.59		-0.47	0.34	
PM	0.80				0.81				
O <sub>3</sub>	0.50		0.70		0.47			0.72	-0.27
SO <sub>2</sub>	0.88				0.86				
HNO <sub>3</sub>	0.86			0.34	0.88				
Ca <sup>2+</sup>	0.59	0.39		0.45	0.60	0.38	0.33		
K <sup>+</sup>	0.29	0.70		0.33	0.36	0.66	0.39		
Na <sup>+</sup>		0.97				0.96			
Mg <sup>2+</sup>		0.95			0.28	0.95			
Cl <sup>-</sup>		0.97				0.98			
NO <sub>3</sub> <sup>-</sup>	0.73	0.48			0.76	0.45			
NH <sub>4</sub> <sup>+</sup>	0.92				0.94				
SO <sub>4</sub> <sup>2-</sup>	0.86				0.88				
Temperature	-	-	-	-			0.94		
Relative humidity	-	-	-	-	-0.26				0.79
Wind speed	-	-	-	-		0.32		0.52	0.49
Precipitation	-	-	-	-					0.79
Component	Combustion/industrial emission	Sea salt	Photochemical production of GOM	Gas-particle partition of Hg	Combustion/industrial emission	Sea salt	Gas-particle partition of Hg	Photochemical production of GOM	Hg wet deposition
Variance explained	37%	25%	11%	9%	30%	20%	10%	10%	9%



Table 8. PCA component loadings (&gt;0.25) of Case 10-C and Case 10-C&amp;M.

Variable	Case 10-C				Case 10-C&M				
	PC1	PC2	PC3	PC4	PC1	PC2	PC3	PC4	PC5
GEM			0.79				0.87		
GOM			0.71	0.33			0.51	-0.51	0.38
PBM			0.48				0.29	-0.62	
O <sub>3</sub>			0.91				0.87		
SO <sub>2</sub>				0.89					0.84
HNO <sub>3</sub>	0.34			0.83	0.33				0.82
Ca <sup>2+</sup>	0.89				0.89				
K <sup>+</sup>	0.77				0.77				
Na <sup>+</sup>		0.99					0.99		
Mg <sup>2+</sup>	0.34	0.93			0.34		0.92		
Cl <sup>-</sup>		0.98					0.97		
NO <sub>3</sub> <sup>-</sup>	0.79				0.80				
NH <sub>4</sub> <sup>+</sup>	0.94				0.94				
SO <sub>4</sub> <sup>2-</sup>	0.90			0.26	0.89				0.26
Temperature	-	-	-	-	0.27		-0.52		0.27
Relative humidity	-	-	-	-				0.74	-0.33
Wind speed	-	-	-	-		0.26	0.52	0.57	
Precipitation	-	-	-	-				0.76	
Component	Combustion emission	Sea salt	Photochemical production of GOM	Industrial source	Combustion emission	Sea salt	Photochemical production of GOM	Hg wet deposition	Industrial source
Variance explained	28%	21%	16%	13%	22%	17%	14%	12%	10%



Table 9. General statistics of speciated Hg with different data treatment options.

a) 2009

Hg form	Case	Percent of missing values	MDL	Percent of values <MDL	Geometric Mean	Median	Mean	Standard deviation
GEM (ng/m <sup>3</sup> )	09	31%		0%	1.37	1.41	1.39	0.28
	09+mean	0%	0.1	0%	1.37	1.37	1.38	0.22
	09+median	0%		0%	1.38	1.41	1.39	0.22
GOM (pg/m <sup>3</sup> )	09	32%		73%	0.57	0.42	1.77	3.98
	09+mean	0%		86%	0.57	0.57	1.39	3.11
	09+median	0%	2	86%	0.51	0.42	1.34	3.12
	09+RM	-		-	-	-	-	-
	09Scale RM	32%		16%	3.91	3.35	5.02	5.49
PBM (pg/m <sup>3</sup> )	09	41%	2	37%	1.79	2.15	2.81	2.71
	09+mean	0%	2	70%	1.79	1.79	2.39	2.14
	09+median	0%	2	28%	1.93	2.15	2.53	2.11
	09+RM	42%	4 (RM)	52%	2.73	3.02	4.69	5.56
	09Scale RM	41%	2	4%	5.52	6.05	6.19	3.15

b) 2010, MDL same as in a)

Hg form	Case	Percent of missing values	Percent of values <MDL	Geometric Mean	Median	Mean	Standard deviation
GEM (ng/m <sup>3</sup> )	10	4%	0%	1.33	1.37	1.34	0.17
	10+mean	0%	0%	1.34	1.37	1.35	0.16
	10+median	0%	0%	1.34	1.38	1.35	0.17
	10+RM	4%	0%	1.33	1.37	1.34	0.17
	10ScaleRM	4%	0%	1.33	1.38	1.34	0.17
GOM (pg/m <sup>3</sup> )	10	4%	96%	0.29	0.26	0.49	0.69
	10+mean	0%	96%	0.27	0.24	0.43	0.63
	10+median	0%	96%	0.27	0.21	0.43	0.63
	10+RM	-	-	-	-	-	-
	10ScaleRM	4%	67%	1.15	1.12	1.40	0.86
PBM (pg/m <sup>3</sup> )	10	4%	51%	1.79	1.92	2.59	2.67
	10+mean	0%	44%	2.08	2.12	3.35	4.04
	10+median	0%	44%	2.08	2.20	3.35	4.04
	10+RM	4%	75%	2.16	2.31	3.08	2.95
	10ScaleRM	4%	1%	6.15	6.38	6.75	3.01



Table 10. Impact of combining or excluding GOM and PBM on PMF factor contributions (>15%) to Hg compounds.

Case	Combustion emission	Industrial sulfur	Photochemistry and re-emission	Sea salt
Case 2009	GOM	PBM	GEM, GOM, and PBM	
Case 09+RM		RM	GEM and RM	
Case 09-RM			GEM	
Case 2010		GOM	GEM, GOM, and PBM	
Case 10+RM			GEM and RM	
Case 10-RM			GEM	



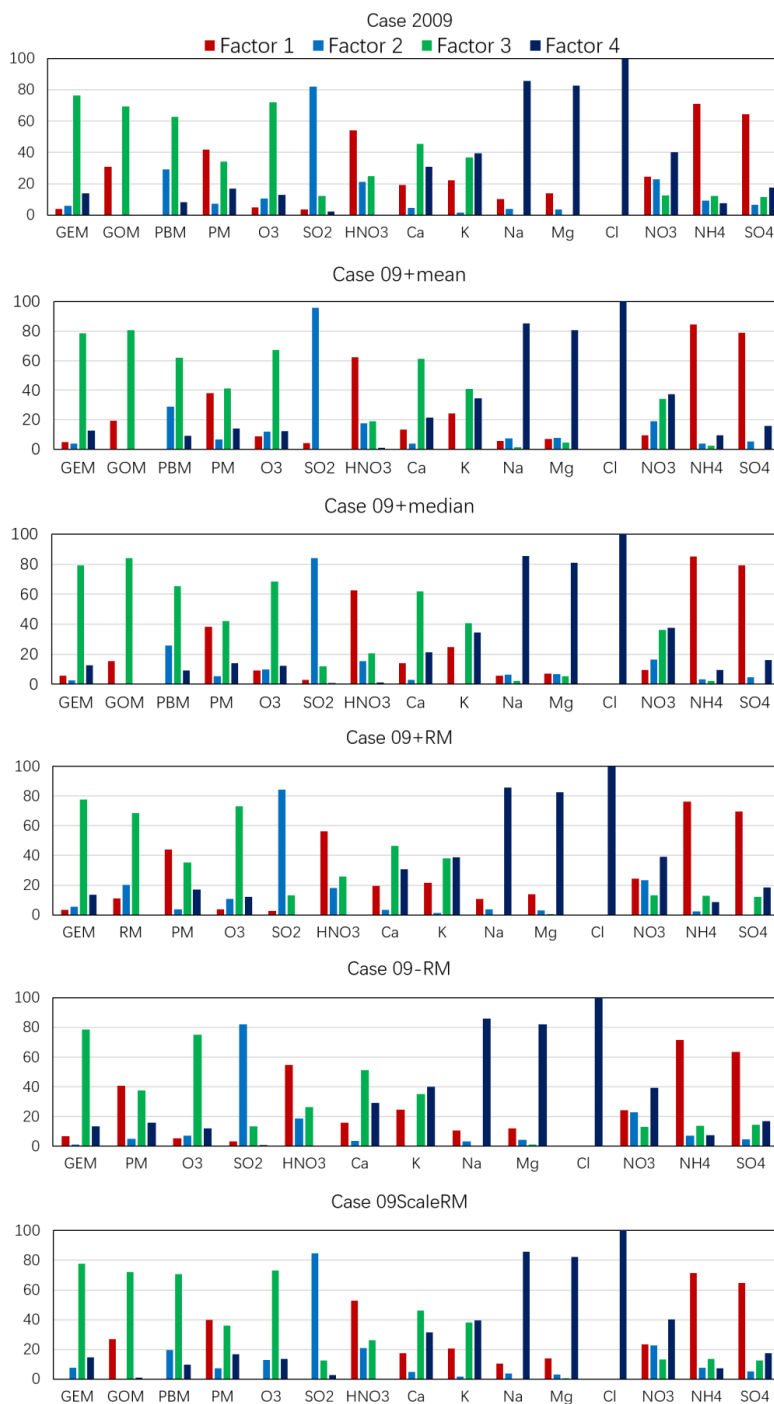


Figure 1. PMF source profiles in percent of concentration, 2009.

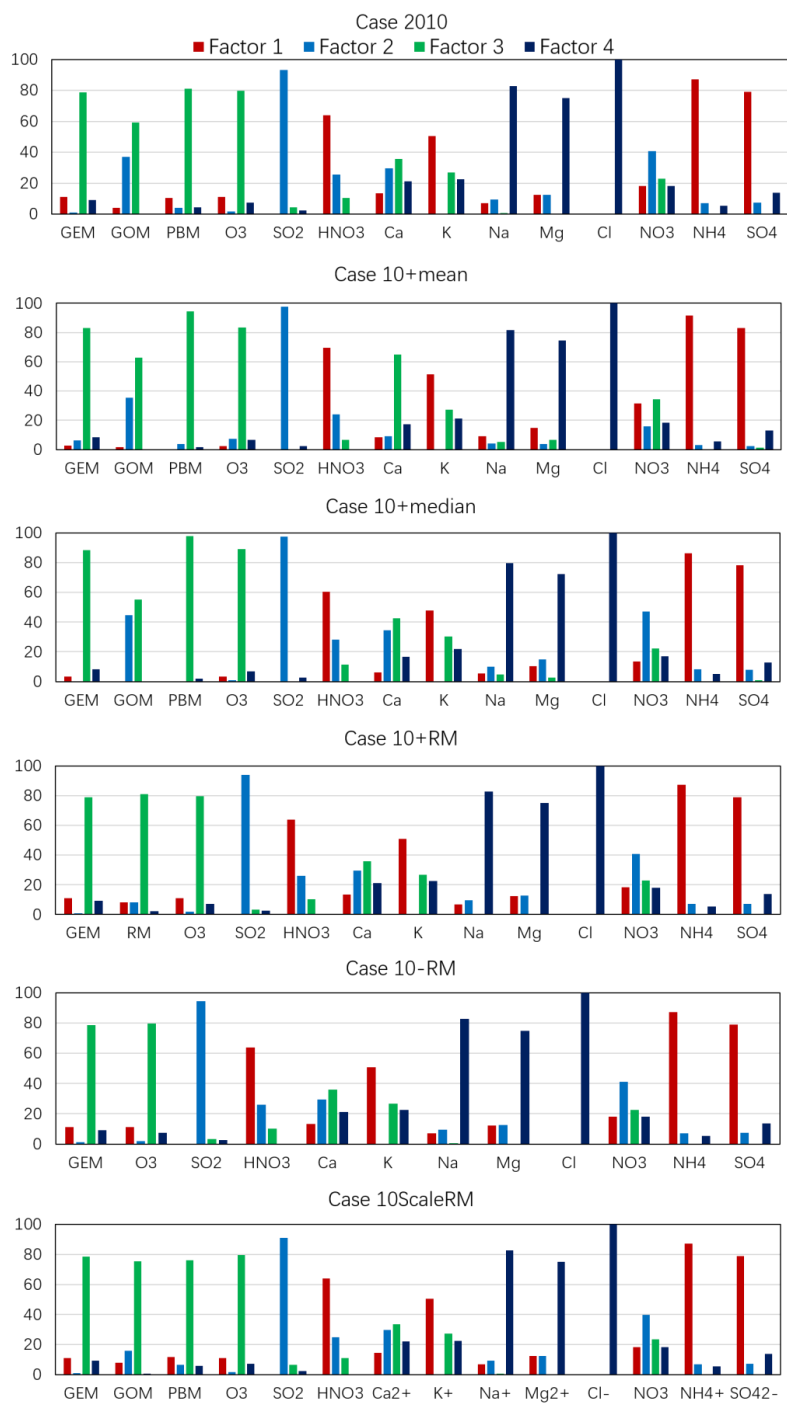


Figure 2. PMF source profiles in percent of concentration, 2010.

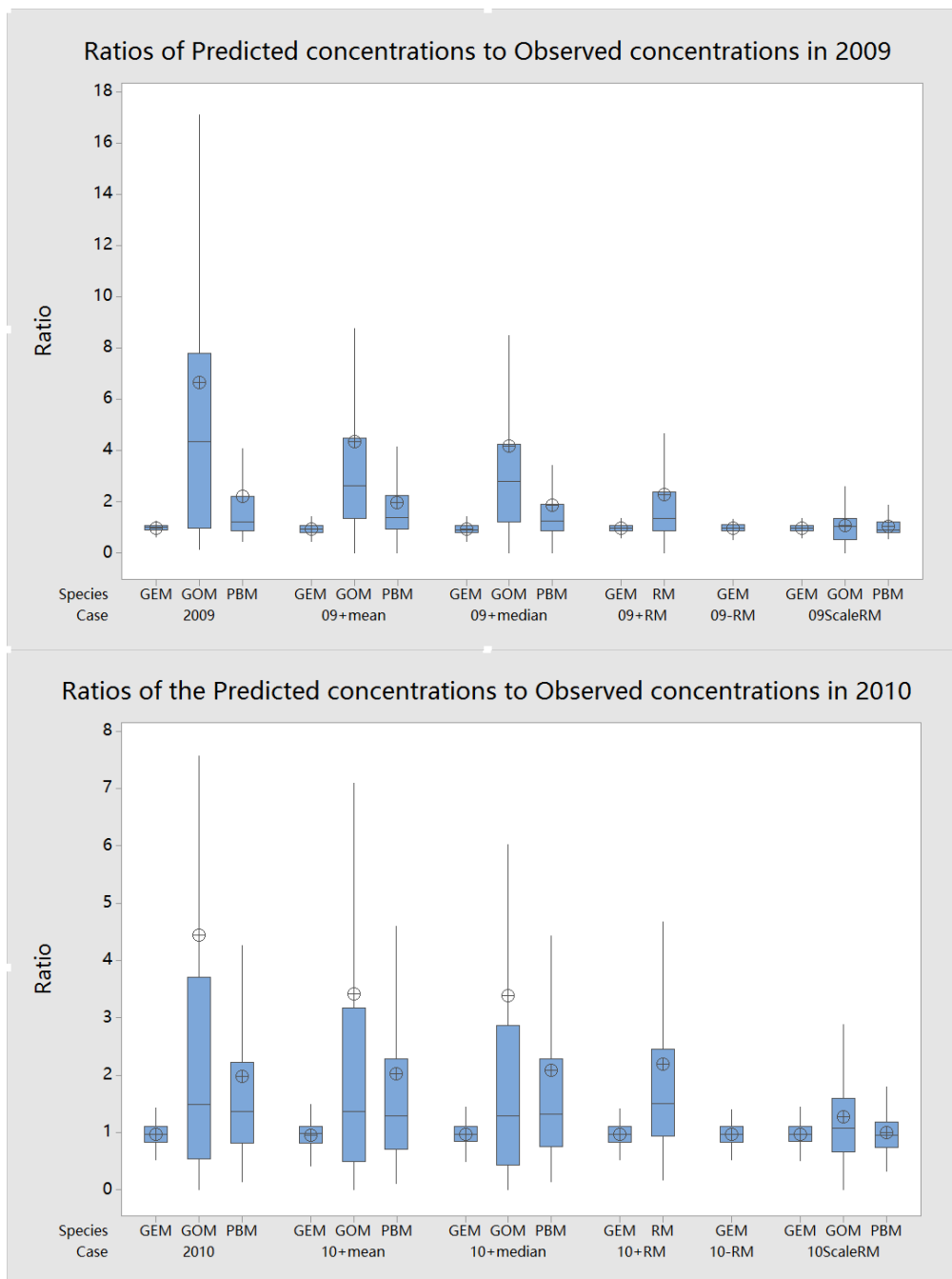


Figure 3. Box plot of predicted to observed concentration ratios (upper whisker- upper 25% of the distribution excluding outliers; interquartile range box - middle 50% of the data; horizontal line in the box - median; lower whisker- lower 25% of the distribution excluding outliers;⊕ - mean).